

GLOBAL JOURNAL OF ENGINEERING SCIENCE AND RESEARCHES IMPACT OF ANGLES ON RADAR ABSORBING MATERIALS USING ALUMINA AND TITANIA FOR X-BAND FREQUENCY RANGE

Preeti*¹ & Vikas Chawla ²

*¹ Research Scholar, Electronics Engineering Department, Mewar University, Chittorgarh, India.

²Professor & HOD, Mechanical Engineering I.K.G.P.T.U. Main Campus, Kapurthala-144001, India

Abstract

Coatings of alumina and titania of two different compositions and at different angles has been developed using plasma spraying method. The surface and cross-sectional morphological characterizations of Al₂O₃ and Al₂O₃/ TiO₂ powders and coatings were done by scanning electron microscope (SEM). The microwave absorbing properties of developed coatings has been observed in X-band (8.2-12.4GHz) frequency range using network analyzer. The reflection loss of Al₂O₃ is -19dB at 10.495GHz with a bandwidth of 0.32Hz whereas reflection loss of Al₂O₃/ TiO₂ 87:13 is -23dB at 10.265GHz with a bandwidth of 0.8GHz. The coatings absorbed 90% of the incident electromagnetic radiation which indicates the material's radar absorbing potential. With appropriate composition and proper spray angle the microwave absorbing properties has been improved.

Keywords: *Plasma Spraying, Radar absorbing materials, Radar Cross Section RCS, coating angle, stealth technology.*

I. INTRODUCTION

With the development in the use of electronic devices over a wide range of military, modern, business and other parts has made another type of pollution such as noise or electromagnetic interference contamination which causes mal capacity of tools. It has been considered to develop microwave absorbing material as it exhibits unique microwave absorbing energy and isolation from electromagnetic compatibility.[1-3]

RAMs have been utilized to absorb RADAR signal sent by opponent to recognize the nearness of aircraft and as microwave signals put unfriendly impact on human wellbeing thus microwave absorbing materials limit the use of home microwave apparatuses. . Since the second world war, there has been expanding interest for radar absorbing materials "stealth" venture for Advanced Technology Bomber and Advanced Technology Fighter [2]. RCS reduction can be obtained by various strategies. The essential strategies utilized are radar absorbing structures, radar straightforward structures, adjustment of geometrical states and utilization of radar retaining materials as surface covering. Application of these coating concepts all types of defense material has been considered. With increase use of radars in battlefield surveillance and weapon homing, also to the traditional air target detection role, means that enhanced techniques for radar camouflage and counter observation must be developed and organized for all types of apparatus.[4,5]

The use of various RCS reduction techniques results in structural changes and also are not cost effective in terms of performance. So, thin radar absorbent coating can be used for improved performance with respect to cost effectiveness.

The reduction RCS of a material, is given by [6-9] the equation is

$$P_r = P_t \frac{G^2 \lambda^2 \sigma}{(4\pi)^3 R^4}$$

Where P_r received power and P_t transmitted power by the antenna respectively, G the antenna gain R the detection range, λ indicates the wavelength and σ is RCS. The equation shows that the detection range varies as the fourth root of the RCS Radar Cross Section. RCS reduction with the reduced detection range has been listed in table 1. A reduction in RCS by 10dB reduces the detection range by almost half.

Table 1

RCS Reduction		Reduced detection range
dB	%	
10	90	0.56 R
15	97	0.42 R
20	99	0.32 R
25	99.7	0.24 R
30	99.9	0.18 R

Electromagnetic absorbers are most often in the form of ceramics or composites. Both alumina and titania can be used to fabricate RAMs [10]. So the microwave absorbing ability and their mechanical properties like morphological (SEM) ,phase transformation by XRD has been studied of thermally sprayed coated samples on alumina substrate.

II. EXPERIMENTAL

1. Materials and Methods

The aluminum substrate was cut into small samples of size 20mm X 15mm X 4mm and the powder compositions used here were 30.18 μm sized Al_2O_3 [99] (Praxair Surface Technologies) and 32 μm sized $\text{Al}_2\text{O}_3/\text{TiO}_2$ [87:13] (Praxair Surface Technologies). The characteristics of commercial powder were summarized as follows
To develop coating plasma spraying process has been used. In this process material in form of powder is molten and then sprayed onto a surface to provide a coating. The powder Material is injected into a very high temperature plasma flame; it has been heated and accelerated with a high velocity. The hot material impacts on the substrate surface and quickly cools form a coating.

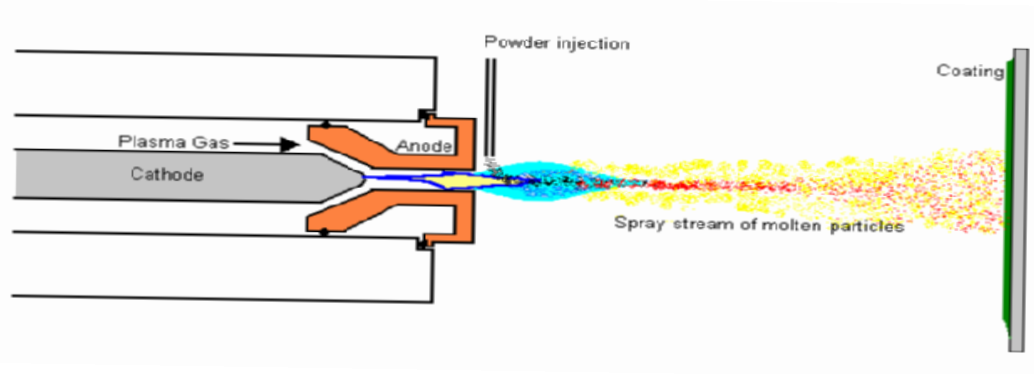


Fig1. Plasma Spraying Process [13]

The Plasma spraying can be used for very high melting point materials such as refractory metals like tungsten and ceramics like zirconia. The coatings developed using plasma spraying are usually much denser, stronger and cleaner than the other thermal spray processes with the exemption of HVOF, HVAF and cold spray processes. [11-14]

The microwave absorption properties effected due to disperse coating angle 30°, 60° and 90° in two different compositions Al_2O_3 99% coded as sample 1, sample 2 and sample 3 respectively and $\text{Al}_2\text{O}_3/\text{TiO}_2$ [87:13] which are coded as sample 4, sample 5 and Sample 6 respectively throughout the study, has been investigated experimentally.

The grit blasting of the samples have been done before coating so as to improve the mechanical adhesion of the coating to substrate, the grit blasting parameters are shown in table 2. The substrate grit blasted samples as shown in fig2 were coated using flame spray at diverse angles by IPM Azadpur , New Delhi India with parameters listed in table 3.

Table 2 Grit Blasting Details

Grit	20 mesh size virgin Brown Alumina
Blasting Air Pressure	2-5 Kg/sq.cm
Surface Roughness	6-10 Ra μm
Working Distance	5-6''
Blasting Angle	900
Pressure Blasting Model	MEC 9182

Table 3: Flame Spray Parameter Details

Process	Flame Spray
Gun	MEC6P Powder Jet
Coating Thickness	Average 100-150 μm
Dye Acetylene Pressure	1-1.1 Kg/cm ²
Dye Acetylene Flow	55 scfh
Angle of coating	900
Oxygen Pressure	2Kg/cm ²
Oxygen Flow	45 scfh
Working Distance	5-6''
Flame Temperature	2000-25000C

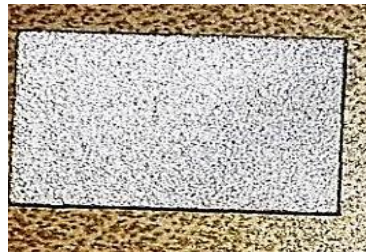


Fig 2 Grit blasted sample



Fig 3 Plasma sprayed samples Al_2O_3 [99] @30°, 60°, 90°

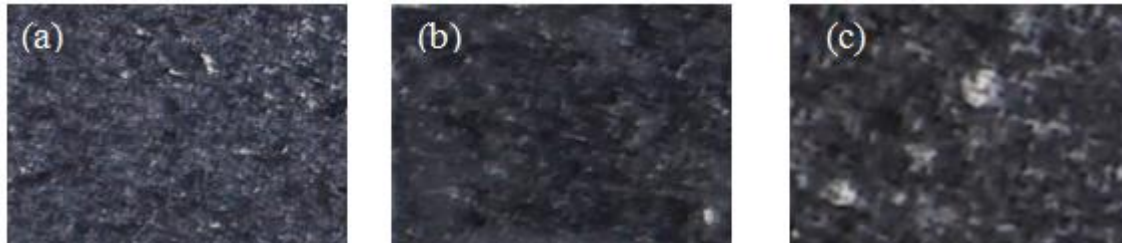


Fig 4 Plasma sprayed samples $Al_2O_3:TiO_2$ [87:13] @30°, 60°, 90°

The images of Plasma sprayed samples were taken with DSLR camera. The camera images does not indicate any changes, so SEM and cross-sectional SEM has been observed for the coated samples. For the cross sectional morphology sample mounting has been done using cold setting compound and cold resin followed by polishing of the surface with successive grade emery papers and velvet clothing using rotating wheel technique at MEC, Jodhpur. The mounted samples were then exposed to scanned electron microscope for cross sectional images of the samples 1,2,3 and samples 4,5,6 as shown by Figure 11 and Figure 12 respectively.

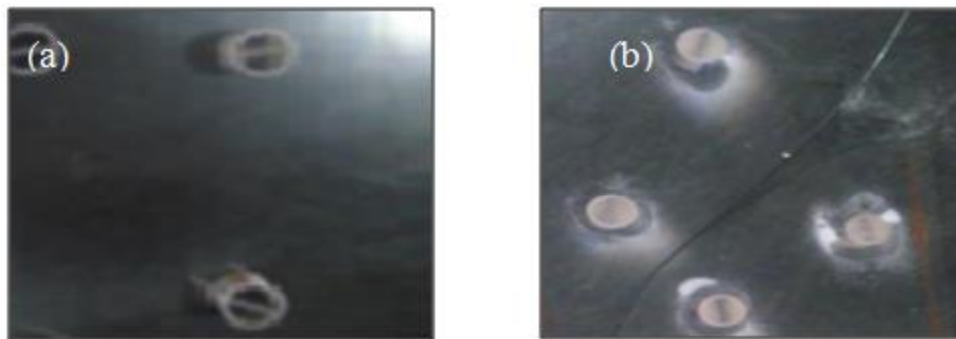


Figure 5: Sample mounting process for cross sectional SEM Micrographs

III. CHARACTERIZATION

Particle morphology with composition of Al_2O_3 [99] and $Al_2O_3:TiO_2$ [87:13] powders as well as coated samples at different spray angles were achieved by Scanning Electron microscopy using SEM, ZEISS, SPRA 55 as shown in figure 6. (a)

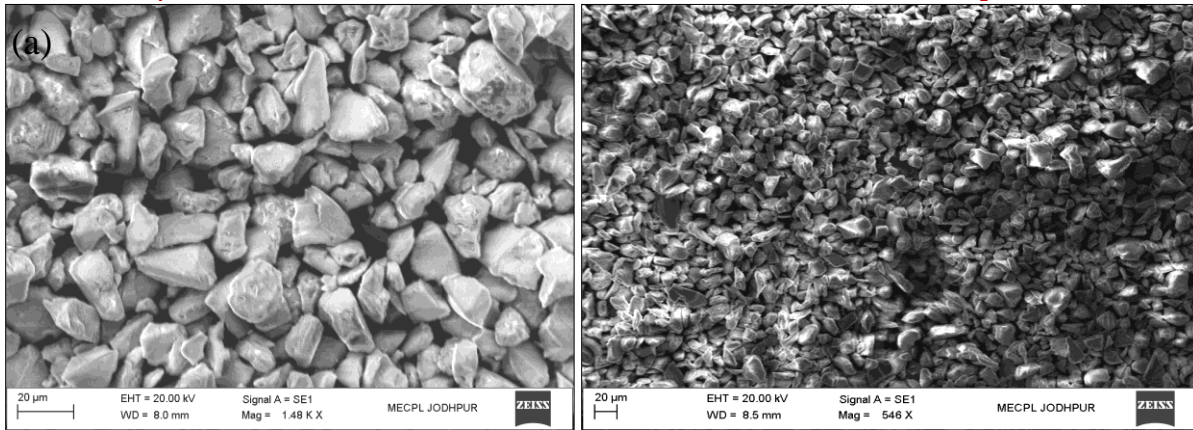


Figure 6: Powder SEM images of $Al_2O_3: TiO_2$ with composition (a) Al_2O_3 [99] and (b) $Al_2O_3: TiO_2$ [87:13]

As already explained in previous research paper on “Mechanical and Electromagnetic Properties of Plasma Sprayed Ceramic Materials” Morphologies of Al_2O_3 [99] and $Al_2O_3:TiO_2$ [87:13] commercially available composite powders are shown Figure 6(a) with particle size in a range of 15–45 μm and mean particle size of 30.18μm whereas the dense solid particles with particle size in a range of 15–43 μm with mean particle size of 32μm specified by Figure6 (b).

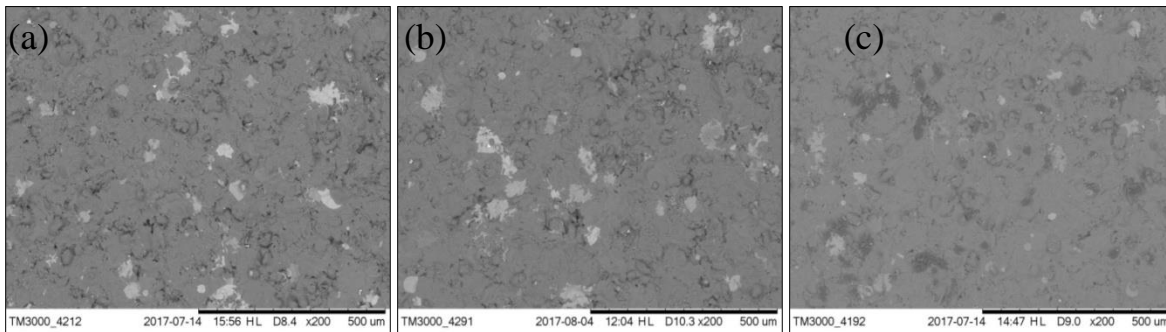


Figure 7: Surface SEM images of coated Al_2O_3 [99] composition at angle (a) 30° (b) 60° (c) 90°

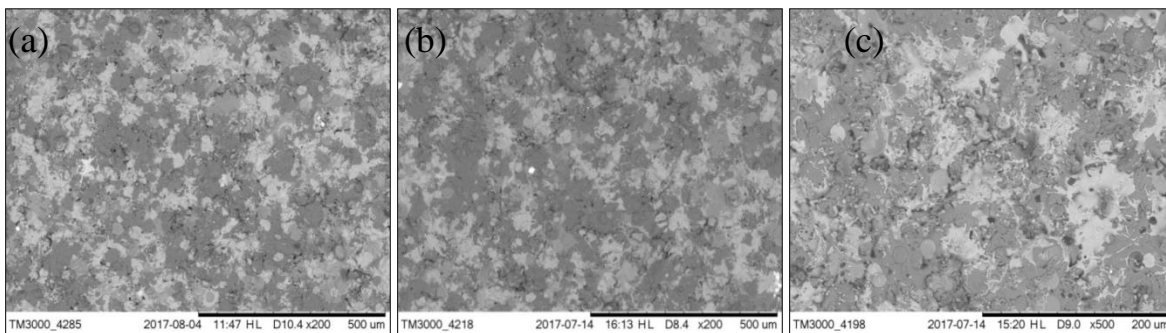


Figure 8: Surface SEM images of coated $Al_2O_3:TiO_2$ [99] composition at angle (a) 30° (b) 60° (c) 90°

In this process ,coating produced were porous and increasing the performance of target by keeping the composite microstructure remain unaltered as shown in fig 6,7 and 8 by SEM micrographs of powders and coated samples.

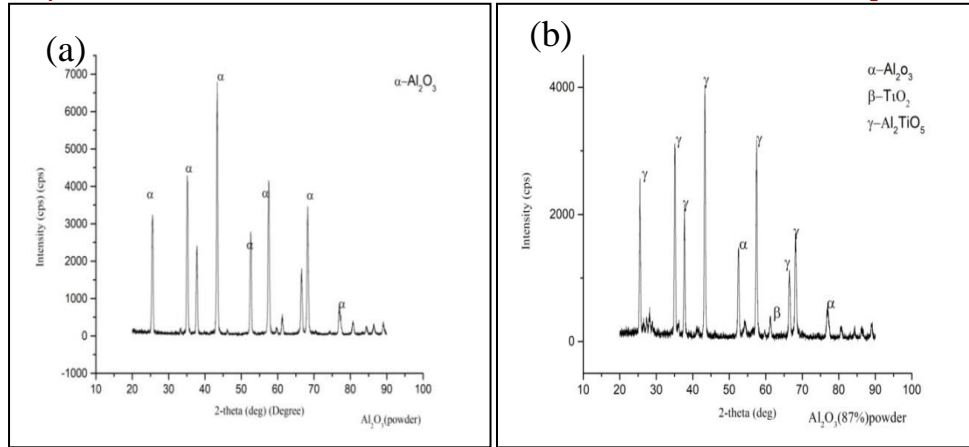


Figure 9: XRD of $Al_2O_3 : TiO_2$ powders with composition (a) Al_2O_3 [99] and (b) $Al_2O_3 : TiO_2$ [87:13]

The content of Al_2O_3 [99] and $Al_2O_3:TiO_2$ [87:13] powders were quantitatively evaluated from XRD plot which was performed at IIT, Delhi. A new phase Al_2TiO_5 appeared due to the combination of alumina Al_2O_3 and titania TiO_2 powders as shown in figure 9 and 10.

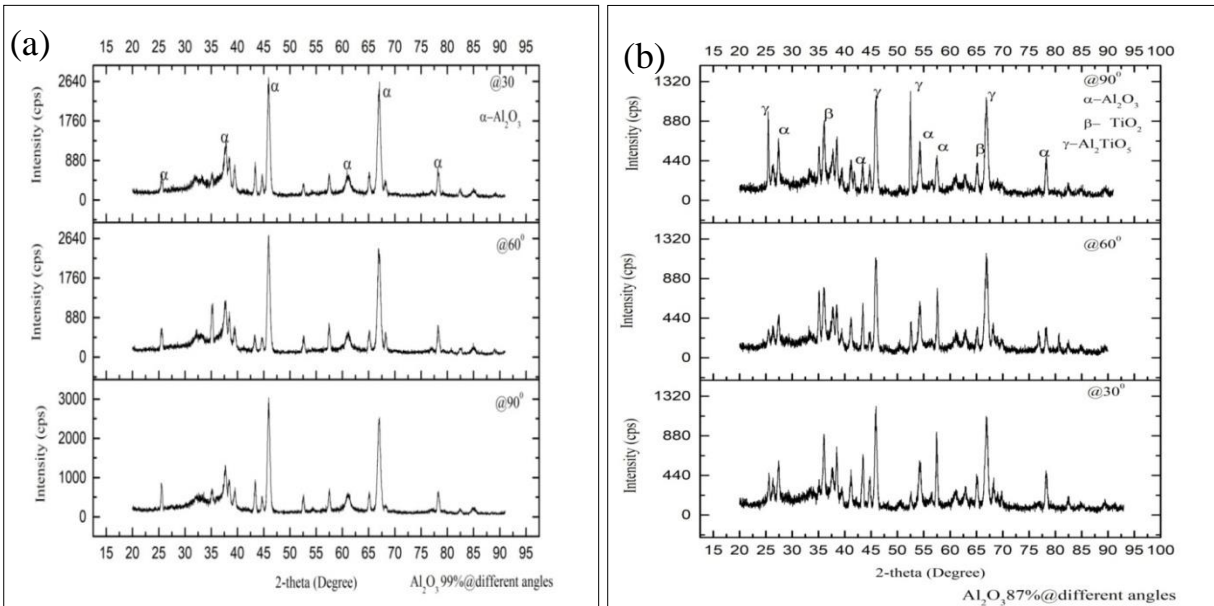


Figure 10: XRD images (a) Al_2O_3 [99] (b) $Al_2O_3 : TiO_2$ [87:13] @different angles

The cross-sectional SEM micrographs of Al_2O_3 [99] and $Al_2O_3:TiO_2$ [87:13] has been indicated in fig 11 and 12 that verified the presence of TiO_2 (13%) in Al_2O_3 .

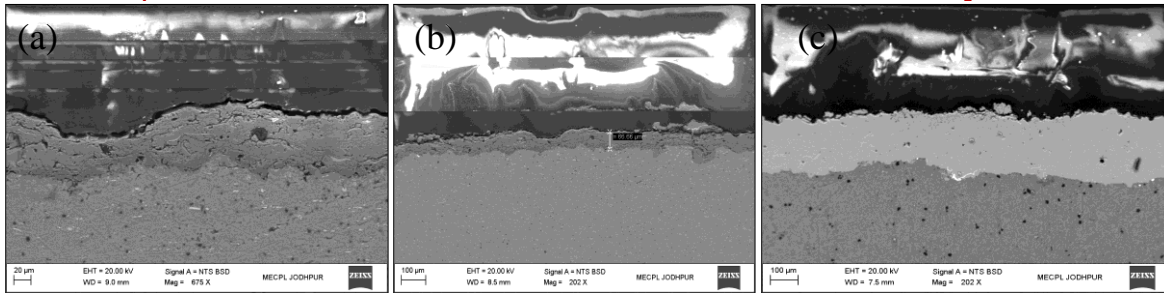


Figure 11: SEM cross sectional of ceramic samples coated with Al_2O_3 [99] compositions at angles (a) 30° (b) 60° and (c) 90° .

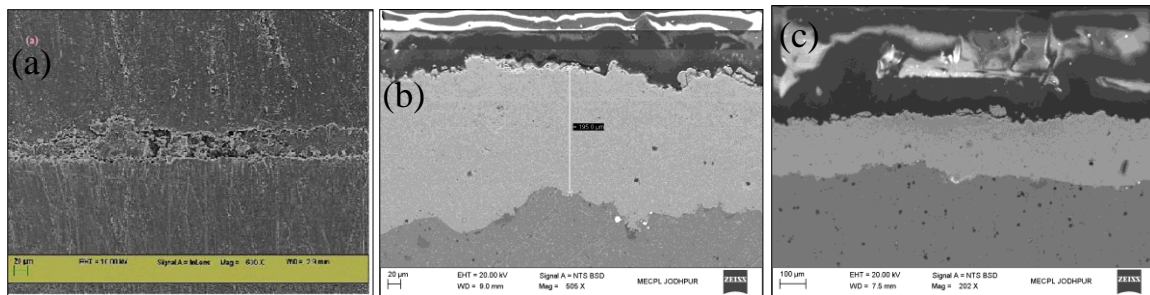


Figure 12: SEM cross sectional of ceramic samples coated with $Al_2O_3:TiO_2$ [87:13] composition at angles (a) 30° (b) 60° and (c) 90° .

The normal size distributions and presence of small particles of TiO_2 on the surface of Al_2O_3 particles showed nanocomposite powders. Figure 6 (b) exposed TiO_2 particle collection on Al_2O_3 as compared to Figure 6 (a) as it contains 99% of Al_2O_3 . Surface morphologies of the coated samples 1, 2, 3 and sample 4,5,6 using flame spraying at above said three angles are shown in Figure 11 and Figure 12 respectively. The surface SEM images of the coated samples have indicated that in both compositions at lower spray angle, the tangential component of the velocity of the in-flight particles during spraying is improved. These strongly control the deformation of the particles into splats at impact with the substrate. At low spray angles elongated splats are formed and orientated in the direction of spraying [15,16].

IV. ELECTRICAL PROPERTIES

The microwave absorption characteristic of material is described [17-20] with power reflection of a plane wave reflected from a metallic surface, aluminum alloy coated by two above said composite ceramics at diverse angles $30^\circ, 60^\circ$ and 90° by plasma spraying. The reflection power or reflectivity of the coating, [21,22] formed for normal incidence, is given as:

$$R = 20 \log(\tau) = 20 \log \left| \frac{Z_i - Z_0}{Z_i + Z_0} \right| \quad (3)$$

τ = Reflection Coefficient, Z_i input impedance and Z_0 Intrinsic Impedance of free space 377Ω .

As per transmission theory the input impedance of absorber Z_i

$$Z_i = \eta \tanh(\gamma d) \quad (4)$$

Where, $\eta = Z_0 \sqrt{\mu/\epsilon}$
and $\gamma = j \frac{2\pi f}{c} \sqrt{\mu\epsilon}$

η, γ, d and μ indicate the intrinsic impedance, propagation constant, thickness, relative complex permittivity and permeability of the composite coating respectively. The velocity of light is represented by c and frequency as f of incident wave.

For the design of microwave absorbing coated samples the two conditions should be considered are.

- 1) Impedance matching: It means that input impedance of the coated samples should be close to free space impedance for the maximum microwave absorption.
- 2) The attenuation of incident wave should fast through the material layer .

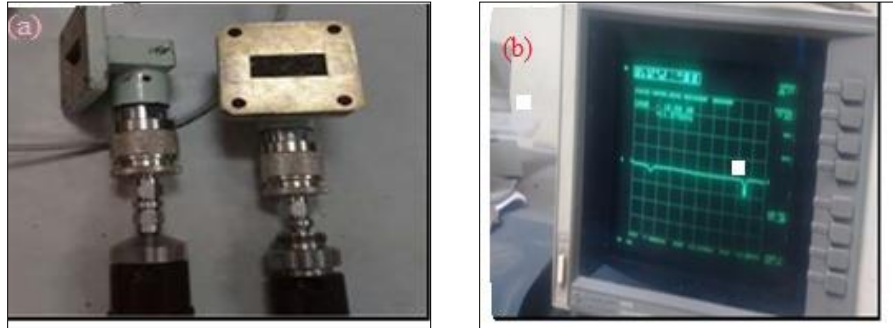


Figure 13. Reflection loss measurement setup (a) Waveguide WR-90 (b) HP87576 Network Analyzer

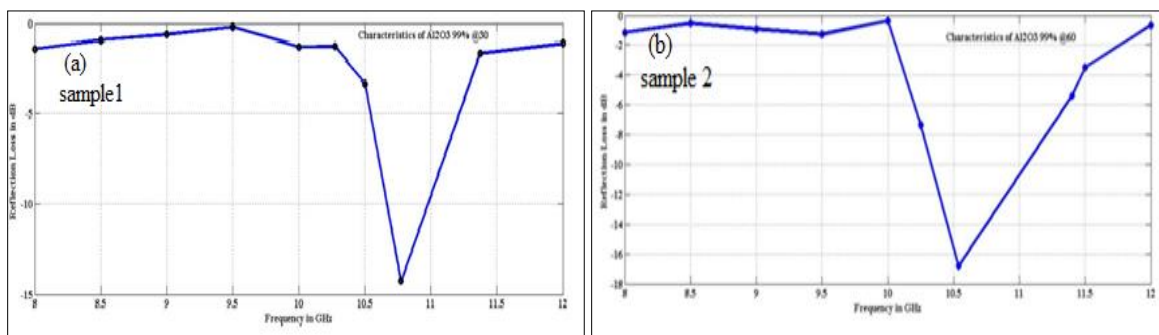
Dielectric probe technique is used to investigate microwave absorbing properties of the coated samples i.e. to measure S_{11} (Reflection Loss) parameters. The reflection loss (electromagnetic absorption) of samples were measured with HP87576 Network Analyzer as shown in fig 13 for frequency range from 8 to 12 GHz (X-band) at Vidyut Yantra Udyog ,Modi Nagar. Before measurement calibration of Network analyzer has been done.

(a) Calibration Phase

The network analyzer must be calibrated before any S-parameter measurements are performed. The system must be allowed to warm up for at least 1 hour before calibration, and the calibration standards must be at ambient room temperature. It is convenient to switch on the analyzer and expose the calibration devices to air before measurements are made.

(b) Calculation Phase

After calibration, coated samples were placed under surface of WR-90 in such a manner so that it covers WR-90. The measurement was done for the X- band range with WR-90. The reflection loss or S_{11} parameter at various points in the X-band range from network analyzer was plotted using MATLAB.



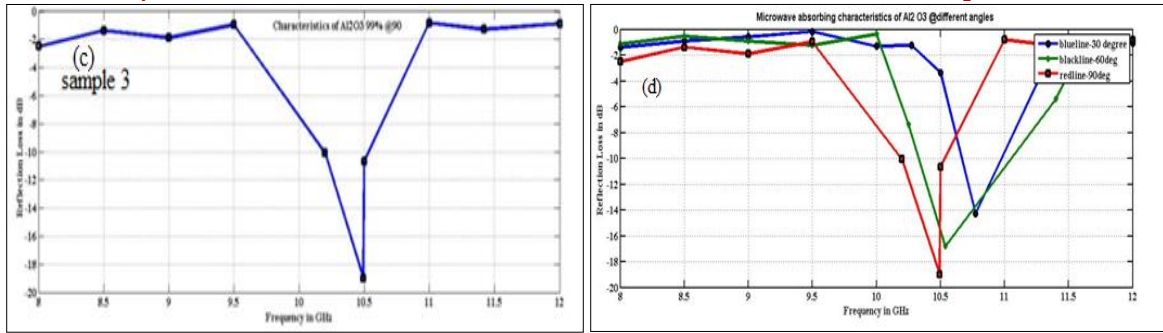


Figure 14: Reflection Loss s_{11} for composition Al_2O_3 [99] coated at angle (a) 30° (b) 60° and (c) 90° (d) combined at different angles

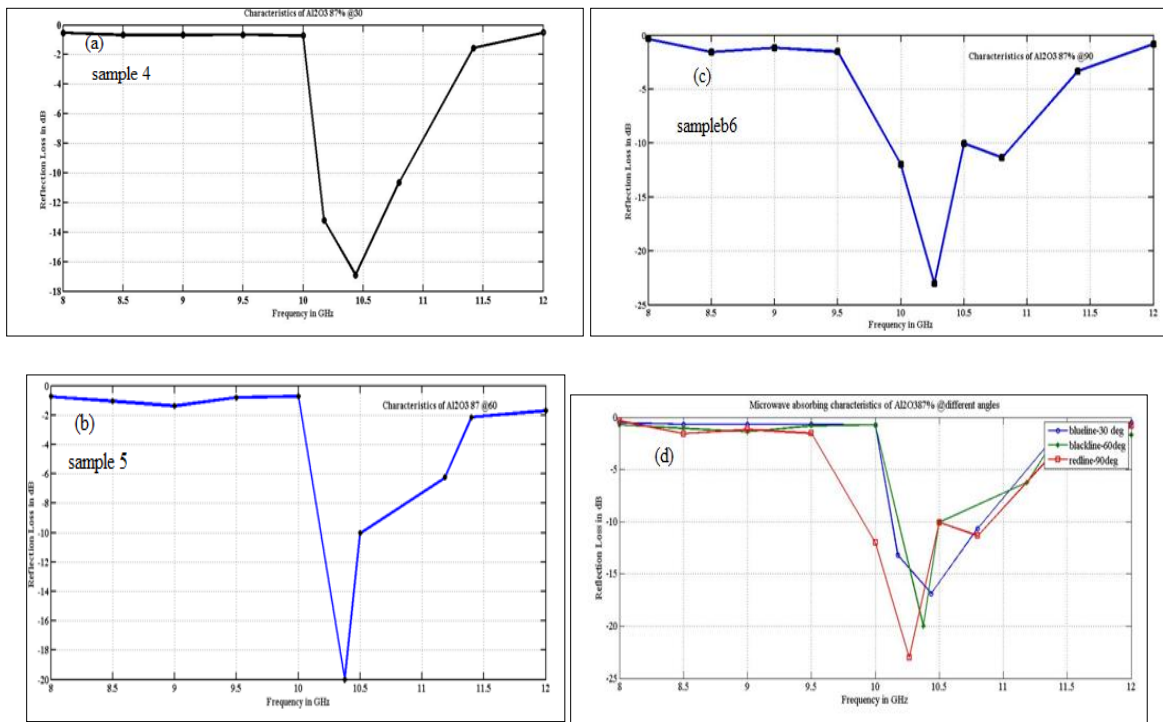


Figure 15: Reflection Loss s_{11} for composition $Al_2O_3 :TiO_2$ [87:13] coated at angle (a) 30° (b) 60° and (c) 90° (d) combined at different angles

It has been observed experimentally that the Sample 1,2 & 3 coated at diverse angles of composition Al_2O_3 [99] results in reflection loss from -10.0dB to -19 dB whereas samples 4,5 and 6 coated ceramic composition $Al_2O_3:TiO_2$ in ratio 87:13 at above said angles produces reflection loss -10.06dB to -23dB measured using wave guide method in X band.

Sample 1 gives >90% absorption with maximum reflection loss of -14.3dB at 10.775GHz as shown in Figure 15(a) Sample2 produces <-10dB reflection loss at 10.537GHz ; as indicated by Figure 14(b). Under same test sample 3 displays maximum reflection loss of -19 dB at 10.495 GHz as indicated by Figure 14(c) i.e band width of 0.5GHz; as shown in Figure 14(c).

Sample 4 exhibits maximum reflection loss of -14.02dB at 9.093GHz; behaves as practical absorber with a band width of 0.725GHz from 10.175 GHz to 10.8 GHz as shown in Figure 15(a). Sample 5 was able to produce <-10dB

loss in a window of 10.375 GHz to 10.5 GHz; band width of 0.125GHz with a maximum reflection loss of -20dB at 10.375GHz as indicated by Figure 15(b). Sample 6 exhibits 90% absorption in a band of 0.8GHz from 10.0GHz to 10.8GHz loss maxima occurs at 10.063GHz of -23dB as shown in Figure 15(c).

Above results has shown that sample 4,5 and 6 with composition of $\text{Al}_2\text{O}_3:\text{TiO}_2$ [87:13] ceramics provide better absorption and enhanced bandwidth than sample 1,2 and 3 Al_2O_3 [99] as shown by S_{11} characteristics of samples plotted simultaneously as shown in fig15 and 16(d). Coated samples in both compositions at lower spray angle showed less absorption and low bandwidth.

V. CONCLUSION

$\text{Al}_2\text{O}_3 / \text{TiO}_2$ coatings with different compositions at different angles were fabricated using plasma spraying and experimentally characterized using network analyzer for X-band. High temperature plasma flame caused phase transformation as indicated by XRD plot.

- It was observed that plasma spraying produced effective RADAR absorbing coatings for sample 6 ($\text{Al}_2\text{O}_3 : \text{TiO}_2$; 87:13 at 90°) with better reflection loss of -23 dB for the frequency range of 10.0-10.8 GHz than as the maximum reflection loss for sample#1 was -19 dB from 10.495 -10.775GHz. With addition of TiO_2 microwave absorbing properties had been improved with better bandwidth.
- For $\text{RL} \leq 10$ dB results 90% microwave absorption and it was observed that sample 3 (Al_2O_3 99% at 90°) showed good absorption properties from 10.495 to 10.775 GHz and maximum reflection loss of -19dB at 10.495GHz, whereas with addition of TiO_2 means sample 6 ($\text{Al}_2\text{O}_3 : \text{TiO}_2$; 87:13 at 90°) with reflection loss of -23 dB at 10.265GHz absorption was monitored from 10.0 to 10.8GHz as shown in fig 15(c) and 16(c).

REFERENCES

1. Skolnik. I Merrill. "Introduction to Radar Systems." 3rd ed. New Delhi (India):Tata Mcgraw-Hill Publishing Company Limited: pp 5-7.
2. http://imagine.gsfc.nasa.gov/docs/science/know_11/emspectrum.html.
3. Balanis CA. *Advanced Engineering Eletromagnetics*. (NYSE)New York: John Wiley Sons.1989
4. Folgueras L.C., Alves, M.A., RezendeM.C. *Microwave absorbing paints and sheets based on carbonyl iron and polyaniline: measurement and simulation of their properties*. JATM .2010; 2(1): 63-70.
5. Sorrentino R. , Bianchi G.: "Microwave and RF Engineering (NYSE)" John Wiley & Sons, Ltd; 2010
6. Aul G. D., Chawla V., and. Vishvakarma S. K, "Microstructure and Microwave Absorption Properties of Flame Sprayed Ceramic Coatings" *International conference on recent trends in engineering science and management ICRTESM-17 22 nd october 2017*.
7. Wang H., Zhu D., Zhou W. and Luoz Fa "Electromagnetic and Microwave Absorption Properties of the Carbonyl Iron/Tic Hybrid Powders in the X Band." *International Journal of Magnetics Electromagnetism*.2016. 2(05): 1-5.
8. Gupta S. ,Aul G., "Agricultural Waste Based-Coco Peat And Coconut Shell Activated Carbon Microwave Absorber, Proceedings" *International Microwave and RF Conference 2016*, 978-1-5090-4685-0/16
9. Kaur, R., Aul, G. D., & Chawla, V. (2015). "Improved reflection loss performance of dried banana leaves pyramidal microwave absorbers" *Progress In Electromagnetics Research M*, 43
10. Dejang, N., Watcharapasorn, A., Wirojupatump, S., Niranatlumpong, P., & Jiansirisomboon, S. (2010). "Fabrication and properties of plasma-sprayed $\text{Al}_2\text{O}_3/\text{TiO}_2$ composite coatings: A role of nano-sized TiO_2 addition." *Surface and Coatings Technology*, 204(9-10), 1651-1657. <https://doi.org/10.1016/j.surfcoat.2009.10.052>
11. Preeti, Chawla V. " Study of Microwave Absorbing Materials - A review." *International Conference on Advancements in Mechanical and Materials Engineering*. 2012 Oct 5-7; Jalandhar, India.
12. Espallargas, "N. Thermal Spray Coating" 2015.; 5(65): 497-509.
13. <https://www.gordonengland.co.uk/ps.htm>
14. Budinski G. Kenneth , Budinski K. Michael "Engineering Materials Properties And Selection." India. Pearson; Ninth edition.

15. Zhu Y., Huang M., Haung J.et.al. "Vaccum Plasma sprayed nanostructured titanium dioxide." 1999; 02: 219-222.
16. Floristán M., Müller P., Gebhardt, A., et.al. "Development and testing of 140GHz absorber coatings for the water baffle of W7-X cryopumps" *Fusion Engineering and Design*. Elsevier Ltd. 2011; 86: 9-11.
17. WangY., Li. T. Zhao L., Hu, Z., Gu, Y. "Research Progress on Nanostructured Radar Absorbing Materials." *EPE*.2011;580-584.
18. Zhao X. , Zhang Z. , Wang L. , Xi K. et.al. "Excellent microwave absorption property of Graphene-coated Fe nanocomposites." *Sci Reports*. 2013; 3: 3421
19. Kim J, Lee S, Kim C. Comparison study on the effect of carbon nano materials for single-layer microwave absorbers in X-band. *CSTE*. 2007; 68(14): 2909-2916.
20. Rosa I M D, Dinescu A, Sarasini F, Sarto M S, Tamburrano A. "Effect of short carbon fibers and MWCNTs on microwave absorbing properties of polyester composites containing nickel-coated carbon fibers" *Composite Science and Technology CSTE*.,2009; 70(1):102-109.
21. Xinwei Ji, X., Zhou Q. Preparation and Research on the Electromagnetic Wave Absorbing Coating with Co-Ferrite and Carbonyl Iron Particles. *Journal of Material Science and Research JMSR*, 2012, 2(2): 35-40.
22. Ganesan L. J. "Reduction of Electromagnetic Interference in Three Phase Squirrel Cage Induction Motor by Coating of Nano Composite Filled Enamel to the Windings of the Motor." *International Journal of Advanced Research in Electrical, Electronics and Instrumentation Engineering IJAREEIE*. Vol. 2, Issue 7, July 2013 978–981.